Am J Cancer Res 2024;14(6):2868-2880
www.ajcr.us /ISSN:2156-6976/ajcr0152179

Original Article

Cdc14B/Cyclin B1 signaling modulates the pathogenesis of sonic hedgehog subtype medulloblastoma

Ting Wang[1*], Shan Wang[2*], Tao Wang[3], Lintao Jia[1], Gang Nan[4], Liang Wang[5]

[1]State Key Laboratory of Cancer Biology, Department of Biochemistry and Molecular Biology, Fourth Military Medical University, Xi'an 710032, Shaanxi, China; [2]Institute of Basic Translational Medicine, Xi'an Medical University, Xi'an 710021, Shaanxi, China; [3]The No. 2 Department of Neurology, Shaanxi Province People's Hospital, Xi'an 710068, Shaanxi, China; [4]Department of Cell Biology, School of Basic Medical Sciences & National Translational Science Center for Molecular Medicine, Fourth Military Medical University, Xi'an 710032, Shaanxi, China; [5]Department of Neurosurgery, Tangdu Hospital, Fourth Military Medical University, Xi'an 710038, Shaanxi, China. [*]Equal contributors.

Received July 12, 2023; Accepted May 13, 2024; Epub June 15, 2024; Published June 30, 2024

Abstract: Medulloblastoma (MB) is a severe malignancy of the central nervous system that predominantly occurs in the cerebellum of children. Overactivation of the sonic hedgehog (Shh) signaling pathway is the primary cause of the development and progression of Shh subtype MB, although the detailed mechanisms underlying this process remain largely elusive. In this study, we discovered that Shh can promote proliferation in MB cells through non-canonical Hedgehog signaling. This involves Shh binding to Patched 1, disrupting its interaction with Cyclin B1, allowing for nuclear translocation of Cyclin B1, and inducing the activation of genes involved in cell division. Furthermore, we observed that deregulation of Cdc14B leads to the stabilization of the Cyclin B1/CDK1 complex in MB cells through activating Cdc25C, a phosphatase known to help maintain Cyclin B1 stability. Our findings highlight the role of Cdc14B/Cdc25C/CDK1/Cyclin B1 in mediating Hedgehog signaling-driven pathogenesis in MB and have implications for identifying potential therapeutic targets.

Keywords: Medulloblastoma, sonic hedgehog (Shh), Cdc14B, Cyclin B1, cell proliferation, cell cycle

Introduction

Medulloblastoma (MB) is one of the most prevalent central nervous system malignancies in children [1]. Characterized by its rapid onset, high malignancy, and propensity for metastasis into the cerebrospinal fluid, MB poses a significant threat to pediatric health. Conventional clinical treatment for MB primarily involves surgical resection combined with radiotherapy and chemotherapy. In recent years, small-molecule inhibitors have also been employed in the clinical management of MB [2, 3]. However, resistance to these inhibitors often develops, underscoring the need for a more comprehensive understanding of MB pathogenesis to improve clinical outcomes [3, 4].

Integrated genomic analysis reveals that MB can be classified into at least four subtypes: Wnt, Sonic hedgehog (Shh), Group3 and Group4; each distinguished by differences in population distribution, phenotype, and clinical symptoms [3, 5]. The Shh subtype accounts for approximately 30% of all MB cases [6]. Mutated genes in this subtype of MB are enriched in the Hedgehog signaling pathway - a crucial regulatory pathway during embryonic development - and aberrant Hedgehog signaling frequently leads to various malignancies [7, 8].

In mammals, the extracellular ligand Shh binds to the cell membrane receptor Patched 1 (Ptch1), thereby releasing it from the inhibitory control exerted by another transmembrane protein, Smoothened (Smo). This release allows Smo to enter the cytoplasm and initiate the recruitment of multiple proteins, including Sufu, to form the Gli processing complex. This complex enables the mature transcription factor Gli to enter the nucleus and activate downstream gene expression, thus playing a critical role in mediating Hedgehog signaling [7, 9].

https://doi.org/10.62347/CVAY8707

In addition to the canonical Shh-Smo-Gli axis described above, Hedgehog ligands can also signal through Type I or Type II atypical pathways [10]. In Type I signaling, Ptch1 forms a complex with Cyclin B1 that is regulated during cell cycle progression. Mutation of the Ptch1 gene or binding of Shh disrupts the association between Ptch1 and Cyclin B1, resulting in the formation of a transcription complex MPF, composed of dephosphorylated CDK1 and Cyclin B1, which then translocates into the nucleus and activates genes required for mitosis [10-12]. The role of this non-classical signaling pathway in MB development remains to be explored.

Evading growth suppressors is a hallmark of cancer, often associated with deregulation of the cell cycle [13]. Abnormal expression or subcellular localization of cell cycle proteins can affect cell proliferation, potentially leading to uncontrolled proliferation and tissue/organ transformation. Maturation-promoting factor (MPF), consisting of Cyclin B1 and CDK1, plays a key role in transitioning from G2 phase to M phase [14, 15]. During G2/M phase checkpoint control, this complex enters the nucleus to activate expression of genes related to proliferation and promote cell division [16]. Cell cycle suppressor Cdc14B has been found to regulate the stability of the Cyclin B1/CDK complex and impede G2/M transition processes [17, 18]. In the present study, we observed aberrant subcellular localization of the key component Cyclin B1 in the non-classical Shh signaling pathway in MB, suggesting its potential involvement in MB pathogenesis. Furthermore, we discovered that reduced expression of Cdc14B in MB cells impairs Cyclin B1 degradation, leading to nuclear accumulation of MPF, resulting in malignant cell proliferation.

Materials and methods

Cell culture and transfection

The human MB cell line Daoy, human embryonic kidney cell line HEK-293T, human lung cancer cell line A549, and mouse embryonic fibroblast cell line NIH3T3 were obtained from the National Collection of Authenticated Cell Cultures (Beijing, China). All cell lines were authenticated by short tandem repeat profiling analysis. All cells were cultured in Dulbecco's Modified Eagle Medium (DMEM, Gibco, Grand Island, NY, USA) supplemented with 10% fetal bovine serum (FBS, Gibco). Cells were routinely grown to 80% confluence at 37°C in a humidified atmosphere containing 5% CO_2. Cells were passaged for a maximum of 2 months, after which new seed stocks were thawed for experimental use. Transfection was performed using Lipofectamine 2000 following the manufacturer's protocol (Invitrogen, Carlsbad, CA, USA).

Small RNAs and lentiviral vectors

Complementary strands of siRNAs were synthesized by GenePharma (Shanghai, China). siRNA sense strand sequences are as follows: siCyclinB1#1, 5'-CCAAACCUUUGUAGUGAAUTT-3'; siCyclinB1#2, 5'-GGUUGUUGCAGGAGACCAUTT-3'. Lentiviral vectors for green fluorescent protein (GFP), wild-type (WT), or mutant Cdc14B were cloned and the recombinant viruses were prepared by GenePharma. Daoy cells were infected with recombinant viruses and selected with 100 μg/mL bleomycin (Sigma-Aldrich, St. Louis, MO, USA) to generate stable clones.

Real-time PCR analysis

Total RNA was extracted from cultured cells or tissues using TRIzol (Invitrogen). cDNA was synthesized from 1.0 μg of total RNA using the Real-time PCR Analysis Kit (Takara, Kusatsu, Shiga, Japan). PCR was performed in triplicate using SYBR Premix Ex Taq (Takara) on a CFX96 Real-Time PCR Detection System (Bio-Rad, Hercules, CA, USA). The $2^{-\Delta\Delta Ct}$ method was used to determine relative gene expression normalized to *ACTB*. The following primers were used for PCR amplification: 5'-AGCCTTCAGCAATGCCAGTGAC-3' and 5'-GTCAGGACCATGCACTGTCTTG-3' for Gli1; 5'-GTCAGAGCCATCAAGACCGAGA-3' and 5'-GCATCTCCACGCCACTGTCATT-3' for Gli2; 5'-TCAGCAAGTGGCTCCTATGGTC-3' and 5'-GCTCTGTTGTCGGCTTAGGATC-3' for Gli3; 5'-TTTCTTTGCGGATGGCAGCACC-3' and 5'-TGTAGCAGGCTATCAGAGTGCC-3' for Cdc14B; and 5'-TCTGGATAATGGTGAATGGACA-3' and 5'-CGATGTGGCATACTTGTTCTTG-3' for Cyclin B1.

Western blotting

Cells were harvested at the indicated times and proteins were extracted for analysis. Nuclear and cytosolic fractions were prepared as described previously [33]. Protein concentra-

tions were quantified using a Pierce BCA Kit (Thermo Fisher, Waltham, MA, USA). Protein samples (20 μg) were separated on SDS/PAGE gels, transferred onto PVDF membranes, and subjected to immunoblot analyses. The following antibodies were used for blotting: Gli1 (2643S, Cell Signaling Technology [CST], Boston, MA, USA), Gli2 (ab26056, Abcam, Cambridge, UK), Gli3 (AF3690, Novus Biologicals, Littleton, CO, USA), Ptch1 (ab109096, Abcam), Cyclin B1 (12231, CST), Cdc14B (ab203675, Abcam), p-Cdc25C (Thr48) (bs-3482R, Bioss, Boston, MA, USA), p-CDK1 (Tyr15) (bs-3092R, Bioss), β-actin (3700, CST), and Lamin B1 (13435, CST). Primary antibodies were stained with horseradish peroxidase (HRP)-linked $F(ab')_2$ goat anti-rabbit and anti-mouse secondary antibodies (ZB-2305, Zhong Shan Jin Qiao, Beijing, China).

Immunoprecipitation

Cell lysates were prepared in lysis buffer (50 mM Tris-HCl [pH 7.4], 150 mM NaCl, 20 mM EDTA, 50 mM NaF, 0.5% NP-40, 0.1 mM Na_3VO_4, 1 mM leupeptin, 20 mg/mL aprotinin, 1 mM dithiothreitol and 1 mM PMSF). Lysates (500 mL) were then incubated overnight at 4°C with 5 μg of the Ptch1 antibody (2468, CST) or an IgG control and 25 μL of Dynabeads® Protein G (Novex, Thermo Fisher). Beads were washed three times with 1 mL of lysis buffer before boiling in sample buffer prior to Western blot analysis.

Cell proliferation assay

Cells were seeded in 96-well plates at a density of 2000 cells per well and serum-starved overnight before culturing in complete medium. Cell proliferation was then evaluated at 0, 24, 48, 72, 96, and 120 hours after medium replacement using Cell Counting Kit-8 (CCK-8) (Boster, Wuhan, China). Briefly, culture medium was replaced with 100 μL of fresh serum-free medium and 10 μL of CCK-8 solution. After incubation at 37°C for 1 hour, absorbance was measured at 450 nm in a Microplate Manager six apparatus (Bio-Rad).

Colony formation assay

Daoy cells in a logarithmic growth phase were dissociated into single cells and seeded onto dishes containing medium with or without the addition of Shh at specified doses (100 ng/mL). The cells were then maintained in a cell culture incubator at 37°C with 5% CO_2 and saturated humidity for 2-3 weeks to allow for colony formation. After fixation with 4% paraformaldehyde, the colonies were stained with 1% methyl violet. Colonies were photographed under a microscope and the number of colonies consisting of more than 50 cells were counted to calculate the efficiency of colony formation. Each clonogenic assay was performed in triplicate.

Immunofluorescence staining

Cells were seeded in 48-well plates, fixed in 4% formaldehyde for 15 minutes at room temperature, and permeabilized with 0.2% Triton X-100 for 5 minutes. Cells were then incubated with a Cyclin B1 antibody (12231, CST) for 1 hour at room temperature. Cells were then washed thrice with PBS and counterstained with the appropriate fluorescent-conjugated secondary antibody. Cells were washed thrice with PBS, and stained with DAPI (Beyotime, Shanghai, China) prior to imaging. Plates were then examined and imaged using a fluorescence microscope (Nikon, Tokyo, Japan).

EdU assay

Cells were seeded in 48-well plates for overnight serum starvation and then cultured in complete medium. Cells were then stained using the BeyoClick™ EdU-488 kit (C0071S, Beyotime) according to manufacturer's protocol and observed with an inverted fluorescence microscope. The ratio of positive nuclei to total nuclei was quantified using ImageJ software (National Institutes of Health, Bethesda, MD, USA).

Animal experiments

All animal protocols were approved by the Animal Care and Welfare Committee of the Fourth Military Medical University. The investigator was not blinded during the experiment. Cells used for in vivo assays were infected with lentivirus expressing firefly luciferase (Genechem, Shanghai, China). Mice were randomly allocated among groups. In total, 5×10^6 cells in 0.1 mL DMEM medium were subcutaneously inoculated into the right posterior flank of male BALB/c nude mice (~20 g, n = 5 per group). Seven days later, the mice were treated with vein injection of saline or Shh (100 ng/g) 3

times/week for 3 weeks. At every week after treatment, the in vivo fluorescence images of the mice after they were anesthetized with isoflurane were acquired using the IVIS imaging system (PerkinElmer, MA, USA). Tumor sizes were measured with a caliper every 3 days after treatment and the volume was calculated using the formula $v = 0.52 \times l \times w^2$, where v is volume, l is length, and w is width.

Immunohistochemistry

For immunohistochemical staining using microarrays of clinical MB tissues (Alenabio, Xi'an, China), slides were de-waxed at 60°C for 30 minutes followed by three 5-minutes washes with xylene, and then hydrated with decreasing concentrations of ethanol (100%, 95% and 80%) for 3 minutes each. Antigen retrieval was performed via microwave heating in sodium citrate buffer. Endogenous peroxidase activity of the tissue was blocked by incubation in 3% hydrogen peroxide for 10 minutes. Sections were then blocked in 5% BSA for 30 minutes and incubated with primary antibodies against Cyclin B1 (PA5-32372, Abcam), (CST), Cdc14B (ab203675, Abcam), p-Cdc25C (Thr48) (bs-3482R, Thermo Fisher) or p-CDK1 (Tyr15) (PA5-121257, Thermo Fisher) at 4°C overnight. Next, the sections were incubated for 30 minutes with the appropriate secondary antibodies, and positive staining was visualized by incubation with 3,3'-diaminobenzidine chromogen for 2-3 minutes. Staining was also performed on tissues isolated from mice that spontaneously develop MB. Briefly, mice were anesthetized with 10% chloral hydrate and perfused through the ascending aorta with 150 mL of normal saline followed by 200 mL of 4% paraformaldehyde. The brain was removed, and the cerebellum was isolated, fixed in 10% formalin, and embedded in paraffin. Five-micron-thick sections were cut and subjected to immunohistochemical staining. All images were obtained with an inverted microscope (Nikon E100, Tokyo, Japan). Staining intensity was scored from 0 to 3 points. The percentage of positively stained cells were scored from 0 to 4. The final score was obtained by multiplying the intensity score and positive proportion score.

Statistics

Data were analyzed using SPSS software. For experiments including qRT-PCR, EdU assays, and cell proliferation assays, statistical significance was evaluated using the two-tailed Student's t-test, with $P < 0.05$ considered significant. For associations between gene expression values, significance was evaluated by the Pearson product-moment correlation coefficient analysis.

Results

Shh promotes MB cell proliferation and xenograft tumor growth

Shh a major ligand that activates the Hedgehog signaling pathway, plays a critical role in both ontogenesis and the development of various malignancies [19, 20]. We investigated the impact of recombinant Shh protein on proliferation of Daoy cells, an MB cell line known to originate from medulloblastoma with an aberrant Hedgehog signaling pathway. CCK-8 assays demonstrated that high-dose Shh treatment significantly enhanced cell growth (**Figure 1A**). EdU staining revealed a significant increase in proliferating Daoy cell number following Shh treatment (**Figure 1B**, **1C**). Additionally, Shh-treated cells exhibited a greater ability to form colonies compared to untreated cells (**Figure 1D**, **1E**). Moreover, intravenous administration of Shh facilitated tumor development in a xenograft MB model (**Figure 1F-I**). These findings suggest that ligand-dependent activation of the Hedgehog signaling pathway promotes MB pathogenesis.

Shh triggers Cyclin B1 nuclear translocation via non-canonical Hedgehog signaling

The Hedgehog signaling pathway regulates gene expression through a family of Gli transcription factors [7]. In Daoy cells, there was modest expression of Gli1/2, but abundant expression of Gli3 at both RNA and protein levels (Supplementary Figure 1A). Treatment with recombinant Shh or a Smo agonist, SAG, did not affect the protein levels of Gli1, Gli2, or Gli3 (Supplementary Figure 1B, 1C). These findings suggest that canonical Hedgehog signaling is not reinforced by Shh or SAG in Daoy cells. Apart from the classical Shh-Smo-Gli axis, Hedgehog ligands can also signal through Type I or Type II atypical pathways [10]. In Type I non-classical signaling, the membrane receptor Ptch1 binds to Cyclin B1 and regulates cell cycle progression [10]. We

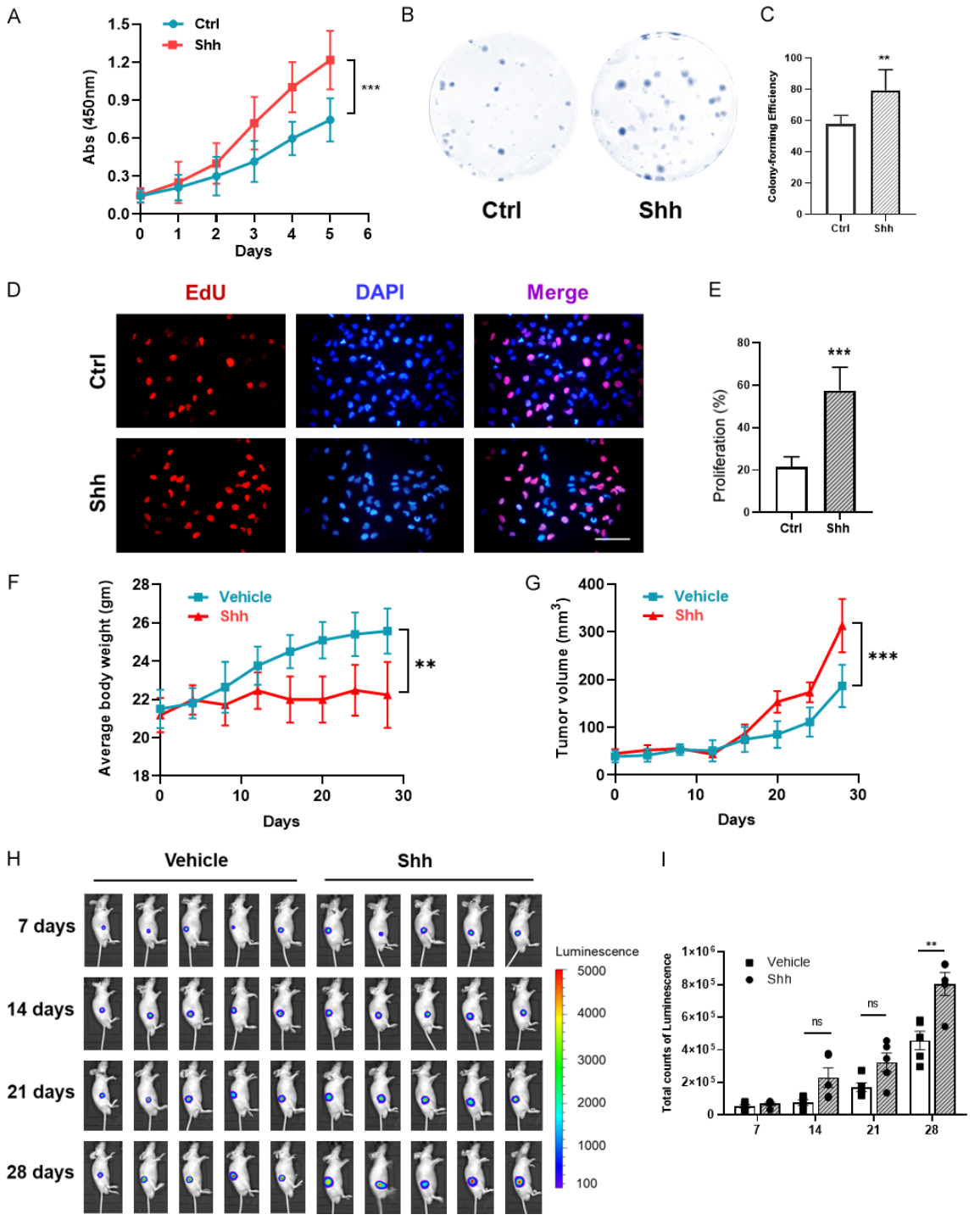

Figure 1. High-dose Shh promotes proliferation of MB cells. (A) Daoy cells were treated with Shh (100 ng/ml) or the solvent and were subjected to CCK-8 assays. (B, C) Daoy cells were treated with Shh (100 ng/ml) or the solvent for 24 h and were subjected to immunofluorescence staining (B) and plate colony formation assays (C). (D, E) Daoy cells were treated with Shh (100 ng/ml) or the solvent for 24 h, and then subjected to plate colony formation assays. (F, G) Quantification of body weight and tumor volume after subcutaneous implantation of ovarian cancer cells. (H, I) Nude mice with subcutaneous medulloblastoma xenografts were imaged in a Xenogen IVIS 200 system and quantified. Data are representative images or are expressed as the means ± SD of three independent experiments. $^{**}P < 0.01$, $^{***}P < 0.001$.

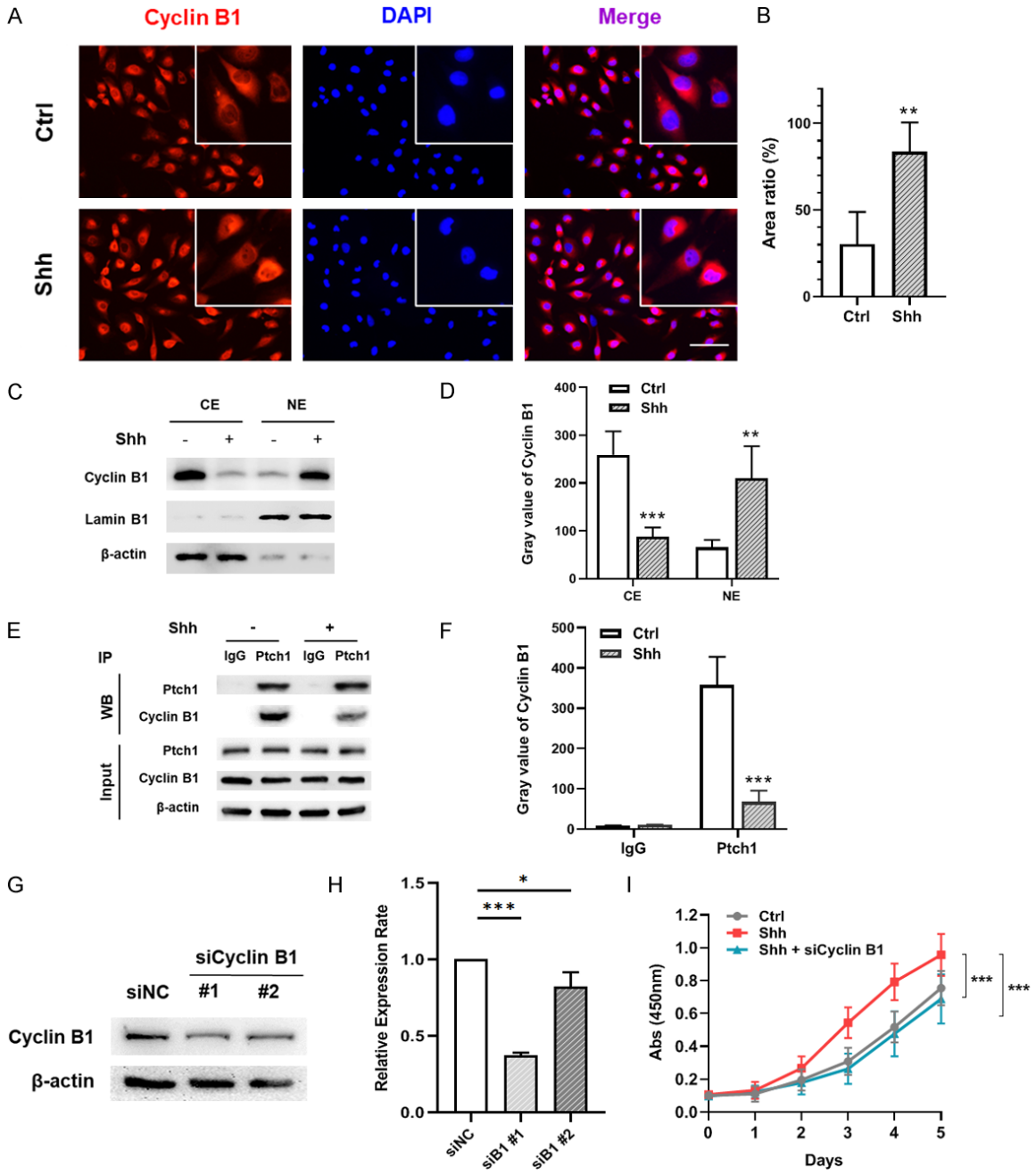

Figure 2. Shh induces nuclear translocation of Cyclin B1 via atypical Hedgehong signaling. A, B. Daoy cells were treated with or without Shh (100 ng/ml) for 24 h, and were subjected to immunofluorescence staining. Scale bar = 10 μm. C, D. Daoy cells were treated with or without Shh (100 ng/ml) for 24 h, and the extracted cytoplasmic (CE) and nuclear (NE) proteins were prepared for Western blot analyses. E, F. Daoy cells were treated with or without Shh (100 ng/ml) for 24 h, and the cell lysates were prepared and used for immunoprecipitation assays. G, H. Daoy cells were transfected with Cyclin B1 siRNAs and subjected to Western blot and qPCR validation for gene silencing. I. siCyclin B1 Daoy cells and control group were both treated with Shh and were performed to CCK8-assays. Data are representative images of three independent experiments. *$P < 0.05$, **$P < 0.01$, ***$P < 0.001$.

therefore investigated the impact of Hedgehog pathway ligand on the subcellular distribution of Cyclin B1. Immunofluorescence staining and Western blot analysis revealed that Shh treatment increased the nuclear localization of Cyclin B1 in Daoy cells (**Figure 2A-D**). Consistent with this observation, immunoprecipitation assays revealed that Shh also reduced binding between Cyclin B1 and Ptch1 in Daoy cells (**Figure 2E**, **2F**). Knockdown of Cyclin B1

decreased cell proliferation induced by Shh in Daoy cells (**Figure 2G-I**). Therefore, Shh likely activates the Type I atypical Hedgehog pathway to promote Cyclin B1 nuclear translocation in MB cells.

Cyclin B1/CDK1 complex stabilization due to Cdc14B deregulation in MB cells

The MPF complex, formed by Cyclin B1 and CDK1, can be activated by phosphorylated cell division cycle 25C (Cdc25C), while Cdc14B dephosphorylates Cdc25C, leading to the complex inactivation and degradation of Cyclin B1 [17]. Consistently, we previously observed downregulation of Cdc14B in MB primary cells compared to cerebellar granule neuron precursors (CGNPs), which are widely accepted as the originators for Shh subtype MB (GEO, accession # GSE85449) [21, 22]. Thus, we investigated whether Cdc14B regulated the total intracellular levels of Cyclin B1 in MB cells. Utilizing a mouse model with spontaneous MB development due to transgenic expression of constitutively active Smo in cerebellar neuron progenitors, we confirmed lower levels of Cdc14B and higher levels of Cyclin B1 in MB tissues compared to CGNPs (**Figure 3A**, **3B**). Overexpression of wild-type Cdc14B, but not the enzymatically inactive mutant, resulted in decreased phosphorylation of Cdc25C (p-Cdc25C) and enhanced CDK1 phosphorylation in Daoy cells, leading to downregulation of Cyclin B1 at the protein level (**Figure 3C-F**). Treatment with the protein synthesis inhibitor cycloheximide (CHX) revealed that Cdc14B promoted the degradation of Cyclin B1 (**Figure 3G**, **3H**). These findings suggest that Cdc14B dysregulation contributes to upregulated Cyclin B1 expression in MB cells.

Cdc14B/Cyclin B1 signaling dictates the proliferation of MB cells

We subsequently investigated the regulatory role of Cdc14B/Cyclin B1 in malignant MB cells. Our findings revealed that overexpression of Cdc14B effectively countered proliferation induced by Shh in Daoy cells, whereas Cyclin B1 overexpression rescued this reduction in growth (**Figure 4A-C**). EdU staining demonstrated that Cyclin B1 reversed the decreased cell division caused by Cdc14B under Shh expression in Daoy cells (**Figure 4D**, **4E**). Moreover, overexpressed Cdc14B significantly reduced the high colony formation rate observed in Shh-treated Daoy cells; however, this effect was reversed upon expression of Cyclin B1 (**Figure 4F**, **4G**). Collectively, our results highlight the critical roles played by Cyclin B1 and Cdc14B as mediators within signal pathways that finely regulate proliferation in MB cells.

Cdc14B/Cyclin B1 signaling modulates MB development in vivo

We next evaluated the involvement of Cdc14B/Cyclin B1 signaling in the development of in vivo MB. Immunohistochemical staining using tissues from the aforementioned spontaneous MB mouse model indicated that Cdc14B and pCDK1 were downregulated while p-Cdc25C and Cyclin B1 levels were elevated in MB compared with the paracancerous tissues (**Figure 5A**, **5B**). Similarly, staining using a tissue microarray of human MB showed lower levels of Cdc14B and pCDK1, and higher levels of p-Cdc25C and Cyclin B1 in Shh subtype compared with other subtypes of MB (**Figure 5C**). Analysis of the IHC scores indicated that Cdc14B levels were reversely correlated with those of Cyclin B1 and p-Cdc25C, but positively associated with pCDK1 level in clinical MB specimens (**Figure 5D**). Collectively, these results suggest that Cyclin B1, which is concurrently regulated by Cdc14B and atypical Hedgehog signaling, contributes to the pathogenesis of Shh subtype of MB.

Discussion

The aberrant Hedgehog pathway has been implicated as a driver of malignancies such as MB and basal cell carcinoma [19]. In Shh subtype MB, transformation occurs in CGNPs due to hyperactivity of Hedgehog signaling, primarily caused by mutations or amplifications affecting genes encoding canonical players within this pathway, including Ptch1 and Smo receptors, cytoplasmic Suppressor of Fused (SUFU), and downstream transcription factors Gli1 and Gli2 [6, 19]. However, non-canonical Hedgehog signaling has also been reported to play crucial roles in MB development [21, 23]. Consistent with these reports, our study demonstrates that Cyclin B1 acts as a key regulator for proliferation, specifically within Shh subtype MB. While Cyclin B1 was activated directly by atypical Hedgehog signaling, the total intracellular levels of Cyclin B1 were also significantly elevated, primarily due to the deficiency of Cdc14B (**Figure 6**). Although further investigations are required to determine whether Cyclin B1 is upregulated in specific phases of the cell cycle,

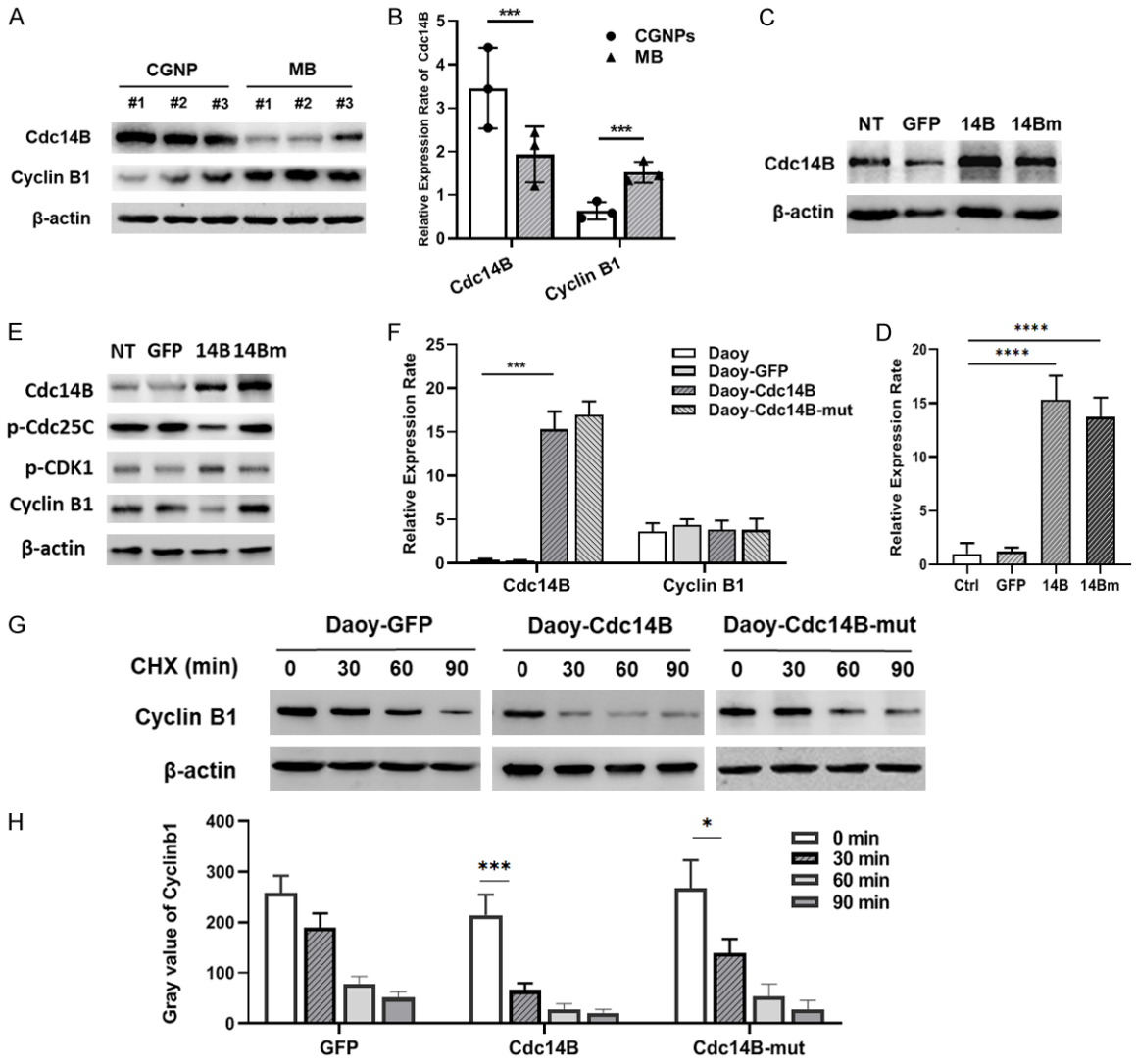

Figure 3. Cyclin B1 was stabilized due to Cdc14B deregulation in MB cells. A, B. MB tissues were isolated from *Neurod2*-SmoA transgenic mice (Jackson Laboratory, Stock #: 008831), and mouse CGNPs were obtained from neonatal mice. The homogenates of MB tissues and the lysates of CGNPs were prepared for Western blot and qPCR analyses. C, D. Daoy cells were transfected with the expressing constructs for GFP, wild-type or the enzyme activity-deficient mutant of Cdc14B, and were subjected to Western blot and qPCR analyses. E. Western blot analyses of p-Cdc25C, p-CDK1 and Cyclin B1 in Daoy cells with different overexpression. F. qPCR analyses of Cdc14B and Cyclin B1 in Daoy cells with different overexpression. G, H. GFP-, Cdc14B- and mutCdc14B- overexpressing Daoy cells were treated with 50 μg/ml CHX for indicated times, and were subjected to Western blot analyses. Data are representative images or are expressed as the means ± SD of three independent experiments. *$P < 0.05$, ***$P < 0.001$, ****$P < 0.0001$.

the Cyclin B1/CDK1 complex has been extensively characterized for its role in promoting significant reorganization of cell architecture necessary for cytokinesis during mitosis [24]. By contrast, we did not observe a significant upregulation of Gli1 or Gli2 by Shh or SAG in Daoy cells, which are well-established cell lines of Shh subtype MB. This suggests that Smo may be constitutively activated or that its signaling to the Gli family transcription factors is disrupted in these cells [25].

Cell division cycle-related genes (*CDC* genes) encode a class of proteins that synergistically orchestrate cell cycle progression [26]. As a member of the Cdc25 phosphatase family, Cdc25C dephosphorylates CDK1 and promotes nuclear entry of the Cyclin B1/CDK1 com-

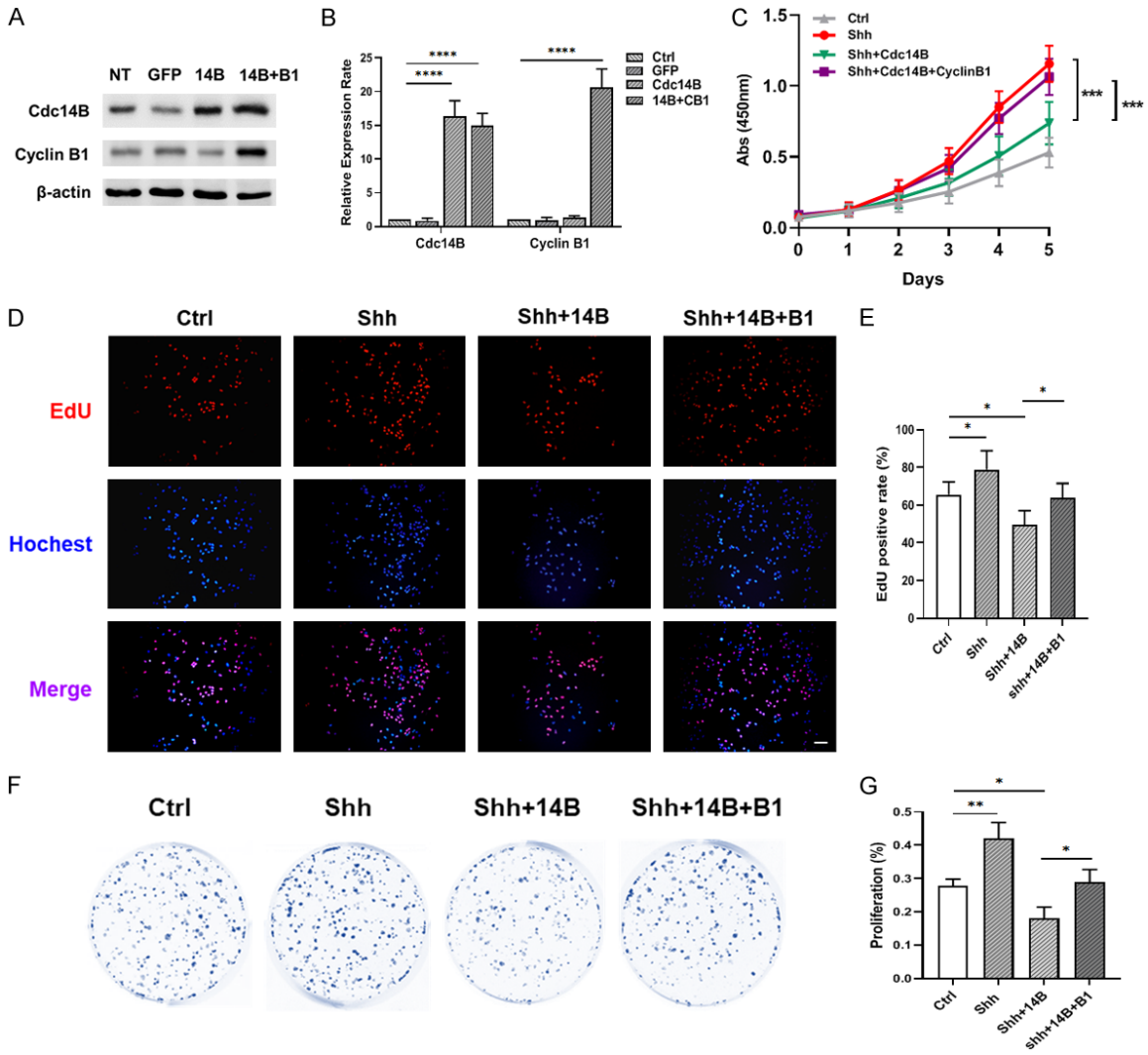

Figure 4. Cdc14B/Cyclin B1 signaling controls MB cell proliferation. (A, B) Cdc14B-overexpression Daoy cells were transfected with expressing constructs for Cyclin B1 and subjected to Western blot and qPCR validation. (C) Different overexpression groups of Daoy cells were treated with Shh (100 ng/ml), with wildtype Daoy cells as control, were subjected to CCK-8 assays for proliferation ability. (D-G) Different overexpression groups of Daoy cells were treated with Shh (100 ng/ml), with wildtype Daoy cells as control, and subjected to immunofluorescence staining (D, E) and plate colony formation assays (F, G). Data are representative images or are expressed as the means ± SD of three independent experiments. Scale bar = 10 μm. **P* < 0.05, ***P* < 0.01, ****P* < 0.001, *****P* < 0.0001.

plex, thus preventing Cyclin B1 degradation and enabling G2/M progression in dividing cells [27]. Cdc25C can also be phosphorylated and activated by CDK1, suggesting that they form a regulatory loop to intensify the signaling required duringM phase entry [28]. Cdc25C activity is negatively regulated by 14-3-3 proteins and kinases including Chk1/2, Wee1, and Myt1 [27, 29]. Consistent with a previous report, we found here that Cdc14B inhibits Cdc25C and expedites the degradation of Cyclin B1, a process inhibited during MB development due to Cdc14B deregulation. These findings are in line with the recent discovery that Cdc14B can counteract the mitosis-specific CDK1-mediated transcriptional program in mammalian cells [30]. Although Cdc14B has been identified as a potential suppressor of various malignancies, further investigations are necessary to understand its regulation in normal and neoplastic cells, e.g., whether it is synthetic lethal with cancer-driving mutations such as aberrant Shh signaling in MB [31].

Despite unveiling a novel mechanism underlying MB pathogenesis, the present study has

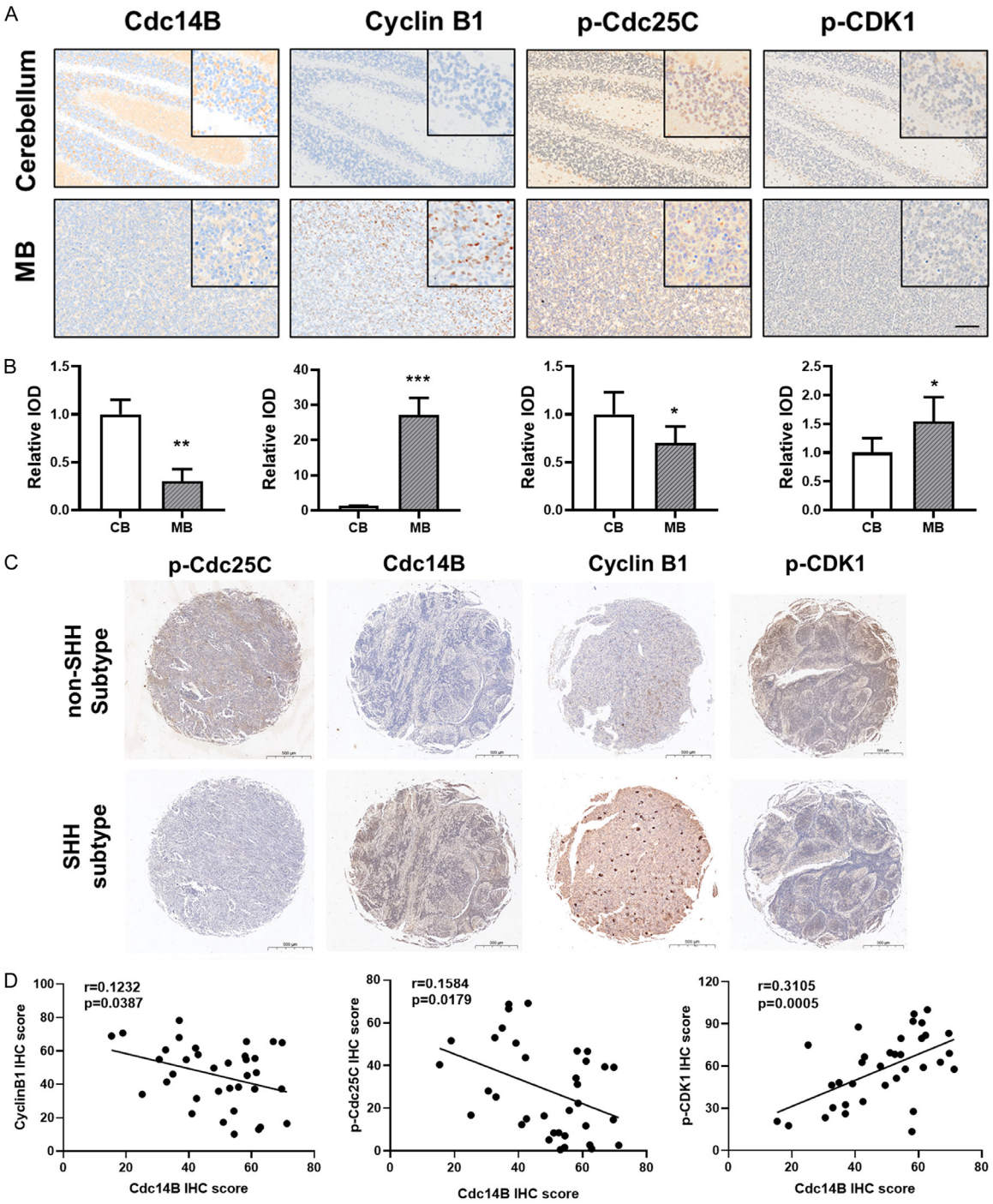

Figure 5. Cdc14B/Cyclin B1 signaling regulates in vivo development of Shh subtype MB. (A, B) MB tissues from *Neurod2*-SmoA transgenic mice were sliced and used for immunohistochemical staining. Scale bar = 10 μm. (C, D) Immunohistochemical staining was performed using microarrays of human MB specimens (C). The staining results were scored and subjected to Pearson correlation analysis (D). **P* < 0.05, ***P* < 0.01, ****P* < 0.001.

several limitations. Firstly, the role of the Cdc14B/Cdc25C/Cyclin B1/CDK1 axis in carcinogenesis needs further validation using additional MB cell lines. Secondly, a more extensive exploration of its involvement in the cell cycle during MB development is warranted, including investigating whether the aforementioned signaling pathway regulates the G2/M

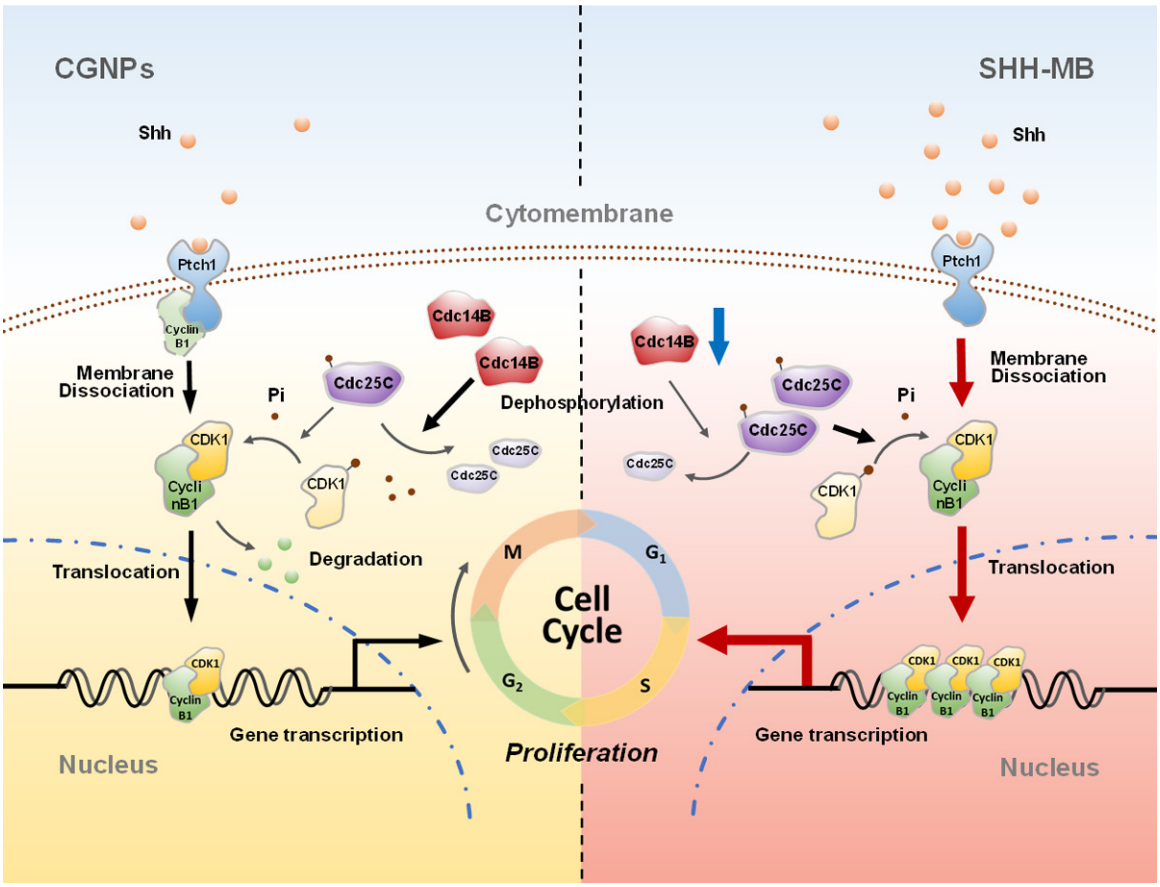

Figure 6. Schematic representation for the regulatory role of Cdc14B/Cyclin B1 in Shh-driven development of MB. Shh engagement on the cognate receptor Patched 1 causes the dissociation of Cyclin B1 from the receptor, allowing its nuclear translocation and transactivation of cell division-related genes. Meanwhile, Cdc14B is deficient in MB cells, which leads to the hyperactivation of its dephosphorylating substrate Cdc25C, reduced phosphorylation of CDK1 and stabilized complex of Cyclin B1/CDK1. The complex thus contributes to excessive proliferation through propelling cell cycle progression.

checkpoint and if inhibiting this pathway or blocking Hedgehog signaling can suppress MB development by inducing cell cycle arrest [32]. Nonetheless, our findings highlight the impact of the atypical Hedgehog pathway on MB occurrence and demonstrate the therapeutic value of targeting Cdc14B and Cyclin B1-mediated cell cycle regulatory machinery in the treatment of Shh subtype MB.

Acknowledgements

This work was supported by National Natural Science Foundation of China (Grant No. 82172910 to L. Jia and Grant No. 81802800 to T. Wang), National Key Laboratory of Human Factors Engineering (Grant No. 61422220-110 to L. Jia), Natural Science Foundation of Shaanxi Province (Grant No. 2023-YBSF-174 to G. Nan) and Natural Science Basic Research Plan in Shaanxi Province of China (Grant No. 2022JM-587 to T. Wang).

Disclosure of conflict of interest

None.

Address correspondence to: Liang Wang, Department of Neurosurgery, Tangdu Hospital, Fourth Military Medical University, No. 569 Xinsi Road, Xi'an 710038, Shaanxi, China. E-mail: drwangliang@126.com; Gang Nan, Department of Cell Biology, School of Basic Medical Sciences & National Translational Science Center for Molecular Medicine, Fourth Military Medical University, No. 169 Changle West Road, Xi'an 710032, Shaanxi, China. E-mail: nanren3033@163.com

References

[1] Parsons DW, Li M, Zhang X, Jones S, Leary RJ, Lin JC, Boca SM, Carter H, Samayoa J, Bettegowda C, Gallia GL, Jallo GI, Binder ZA, Nikolsky Y, Hartigan J, Smith DR, Gerhard DS, Fults DW, VandenBerg S, Berger MS, Marie SK, Shinjo SM, Clara C, Phillips PC, Minturn JE, Biegel JA, Judkins AR, Resnick AC, Storm PB, Curran T, He Y, Rasheed BA, Friedman HS, Keir ST, McLendon R, Northcott PA, Taylor MD, Burger PC, Riggins GJ, Karchin R, Parmigiani G, Bigner DD, Yan H, Papadopoulos N, Vogelstein B, Kinzler KW and Velculescu VE. The genetic landscape of the childhood cancer medulloblastoma. Science 2011; 331: 435-439.

[2] DeSouza RM, Jones BR, Lowis SP and Kurian KM. Pediatric medulloblastoma - update on molecular classification driving targeted therapies. Front Oncol 2014; 4: 176.

[3] Fang FY, Rosenblum JS, Ho WS and Heiss JD. New developments in the pathogenesis, therapeutic targeting, and treatment of pediatric medulloblastoma. Cancers (Basel) 2022; 14: 2285.

[4] Kristensen BW, Priesterbach-Ackley LP, Petersen JK and Wesseling P. Molecular pathology of tumors of the central nervous system. Ann Oncol 2019; 30: 1265-1278.

[5] Li KK, Lau KM and Ng HK. Signaling pathway and molecular subgroups of medulloblastoma. Int J Clin Exp Pathol 2013; 6: 1211-1222.

[6] Northcott PA, Korshunov A, Pfister SM and Taylor MD. The clinical implications of medulloblastoma subgroups. Nat Rev Neurol 2012; 8: 340-351.

[7] Briscoe J and Therond PP. The mechanisms of Hedgehog signalling and its roles in development and disease. Nat Rev Mol Cell Biol 2013; 14: 416-429.

[8] Ramaswamy V and Taylor MD. Medulloblastoma: from myth to molecular. J Clin Oncol 2017; 35: 2355-2363.

[9] Parisi MJ and Lin H. The role of the hedgehog/patched signaling pathway in epithelial stem cell proliferation: from fly to human. Cell Res 1998; 8: 15-21.

[10] Robbins DJ, Fei DL and Riobo NA. The Hedgehog signal transduction network. Sci Signal 2012; 5: re6.

[11] Barnes EA, Kong M, Ollendorff V and Donoghue DJ. Patched1 interacts with cyclin B1 to regulate cell cycle progression. EMBO J 2001; 20: 2214-2223.

[12] Takizawa CG and Morgan DO. Control of mitosis by changes in the subcellular location of cyclin-B1-Cdk1 and Cdc25C. Curr Opin Cell Biol 2000; 12: 658-665.

[13] Hanahan D. Hallmarks of cancer: new dimensions. Cancer Discov 2022; 12: 31-46.

[14] Grallert A, Patel A, Tallada VA, Chan KY, Bagley S, Krapp A, Simanis V and Hagan IM. Centrosomal MPF triggers the mitotic and morphogenetic switches of fission yeast. Nat Cell Biol 2013; 15: 88-95.

[15] Niwa O and Yanagida M. Universal and essential role of MPF/cdc2+. Nature 1988; 336: 430.

[16] Matthews HK, Bertoli C and de Bruin RAM. Cell cycle control in cancer. Nat Rev Mol Cell Biol 2022; 23: 74-88.

[17] Tumurbaatar I, Cizmecioglu O, Hoffmann I, Grummt I and Voit R. Human Cdc14B promotes progression through mitosis by dephosphorylating Cdc25 and regulating Cdk1/cyclin B activity. PLoS One 2011; 6: e14711.

[18] Bai GY, Choe MH, Kim JS and Oh JS. Mis12 controls cyclin B1 stabilization via Cdc14B-mediated APC/C(Cdh1) regulation during meiotic G2/M transition in mouse oocytes. Development 2020; 147: dev185322.

[19] Lazcano P, Schmidtke MW, Onu CJ and Greenberg ML. Phosphatidic acid inhibits inositol synthesis by inducing nuclear translocation of kinase IP6K1 and repression of myo-inositol-3-P synthase. J Biol Chem 2022; 298: 102363.

[20] Onishi H and Katano M. Hedgehog signaling pathway as a therapeutic target in various types of cancer. Cancer Sci 2011; 102: 1756-1760.

[21] Ruch JM and Kim EJ. Hedgehog signaling pathway and cancer therapeutics: progress to date. Drugs 2013; 73: 613-623.

[22] Northcott PA, Robinson GW, Kratz CP, Mabbott DJ, Pomeroy SL, Clifford SC, Rutkowski S, Ellison DW, Malkin D, Taylor MD, Gajjar A and Pfister SM. Medulloblastoma. Nat Rev Dis Primers 2019; 5: 11.

[23] Zhang Y, Wang T, Wang S, Xiong Y, Zhang R, Zhang X, Zhao J, Yang AG, Wang L and Jia L. Nkx2-2as suppression contributes to the pathogenesis of sonic hedgehog medulloblastoma. Cancer Res 2018; 78: 962-973.

[24] Wang W, Shiraishi R and Kawauchi D. Sonic hedgehog signaling in cerebellar development and cancer. Front Cell Dev Biol 2022; 10: 864035.

[25] Mohamed TMA, Ang YS, Radzinsky E, Zhou P, Huang Y, Elfenbein A, Foley A, Magnitsky S and Srivastava D. Regulation of cell cycle to stimulate adult cardiomyocyte proliferation and cardiac regeneration. Cell 2018; 173: 104-116, e12.

[26] Yao YL, Wang YX, Yang FC, Wang C, Mao M, Gai QJ, He J, Qin Y, Yao XX, Lan X, Zhu J, Lu HM, Zeng H, Yao XH, Bian XW and Wang Y. Targeting

AKT and CK2 represents a novel therapeutic strategy for SMO constitutive activation-driven medulloblastoma. CNS Neurosci Ther 2022; 28: 1033-1044.

[27] Moriya H, Shimizu-Yoshida Y and Kitano H. In vivo robustness analysis of cell division cycle genes in Saccharomyces cerevisiae. PLoS Genet 2006; 2: e111.

[28] Liu K, Zheng M, Lu R, Du J, Zhao Q, Li Z, Li Y and Zhang S. The role of CDC25C in cell cycle regulation and clinical cancer therapy: a systematic review. Cancer Cell Int 2020; 20: 213.

[29] Trunnell NB, Poon AC, Kim SY and Ferrell JE Jr. Ultrasensitivity in the regulation of Cdc25C by Cdk1. Mol Cell 2011; 41: 263-274.

[30] Tan T, Wu C, Liu B, Pan BF, Hawke DH, Su Z, Liu S, Zhang W, Wang R, Lin SH and Kuang J. Revisiting the multisite phosphorylation that produces the M-phase supershift of key mitotic regulators. Mol Biol Cell 2022; 33: ar115.

[31] Dietachmayr M, Rathakrishnan A, Karpiuk O, von Zweydorf F, Engleitner T, Fernandez-Saiz V, Schenk P, Ueffing M, Rad R, Eilers M, Gloeckner CJ, Clemm von Hohenberg K and Bassermann F. Antagonistic activities of CDC14B and CDK1 on USP9X regulate WT1-dependent mitotic transcription and survival. Nat Commun 2020; 11: 1268.

[32] Kim Y, Choi JW, Lee JH and Kim YS. Loss of CDC14B expression in clear cell renal cell carcinoma: meta-analysis of microarray data sets. Am J Clin Pathol 2014; 141: 551-558.

[33] Youn YH, Hou S, Wu CC, Kawauchi D, Orr BA, Robinson GW, Finkelstein D, Taketo MM, Gilbertson RJ, Roussel MF and Han YG. Primary cilia control translation and the cell cycle in medulloblastoma. Genes Dev 2022; 36: 737-751.

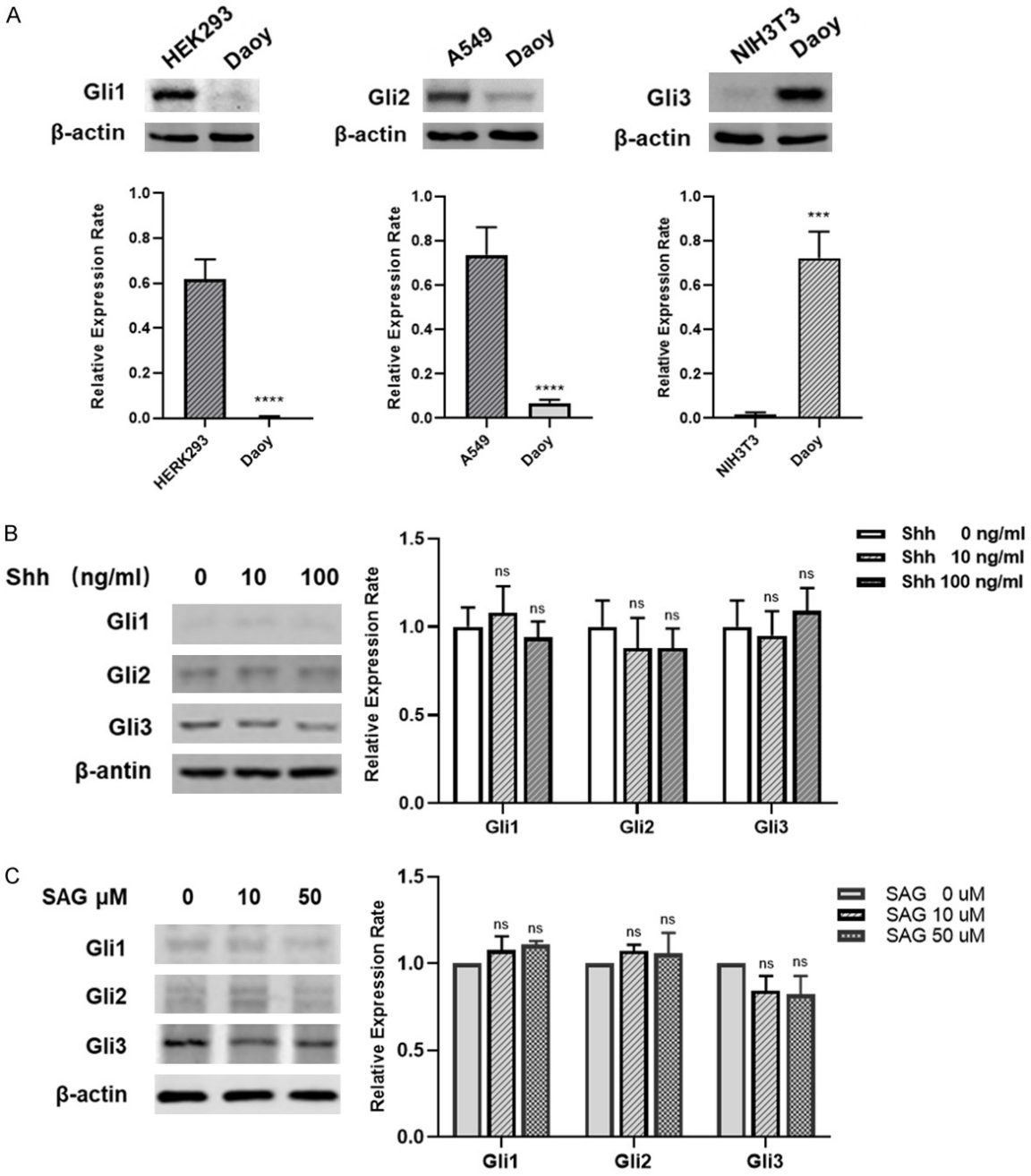

Supplementary Figure 1. Shh and SAG fail to upregulate Gli1/2 in Daoy cells. A. Western blot analyses using the lysates of the indicated cell lines. B, C. Daoy cells were treated with indicated concentrations of Shh or SAG, and were subjected to Western blot analyses. Data are representative images or are expressed as the means ± SD of three independent experiments. n.s., non-significant.